Open-loop sustained chaos and control: A manifold approach

Ira B. Schwartz and Ioana Triandaf
Nonlinear System Dynamics Section, U.S. Naval Research Laboratory, Code 6792, Plasma Physics Division, Washington, D.C. 20375-5000

Riccardo Meucci
Istituto Nazionale di Ottica Applicata, 50125 Florence, Italy

Thomas W. Carr
Department of Mathematics, Southern Methodist University, Dallas, Texas 75275-0156
(Received 2 April 2002; published 27 August 2002)

We present a general method for preserving chaos in nonchaotic parameter regimes as well as preserving periodic behavior in chaotic regimes using a multifrequency phase control. The systems considered are nonlinear systems driven at a base frequency. Multifrequency phase control is defined as the addition of small subharmonic amplitude modulation coupled with a phase shift. By implementing multifrequency control, stable and unstable manifold intersections in postcrisis regimes may be manipulated to sustain chaos as well as to sustain periodic behavior. The theory and a preliminary experiment are demonstrated for a CO_2 driven laser.

DOI: 10.1103/PhysRevE.66.026213 PACS number(s): 05.45.Gg, 42.55.−f, 42.62.−b

I. INTRODUCTION

In the present paper we present an open-loop procedure of sustaining chaos in dynamical systems in regions where the chaotic attractor disappears. Chaos can be a desirable behavior in biological [1], mechanical [2], electrical [3], and optical systems [4]. In mechanics, small amplitude chaos, where the energy is spread over several modes, may be preferable to high amplitude resonant behavior [5,6]. Excellent critical examples of sustaining chaos occur in population models in which the disappearance of chaos leads to the extinction of one of the species in the model, and power systems in which voltage collapse is explained as a crisis in a chaotic attractor [3]. Sustained chaos is also used in encoding information in nonlinear optical communications schemes [4] in diagnosing biological dynamics of pathological phenomena [7,1,8].

Once chaotic behavior appears as an attractor, chaos typically and dramatically disappears as a result of a crisis, which is an abrupt change from chaos to periodic behavior at a critical parameter value of the system [9]. The crisis occurs when the chaotic attractor collides with the stable manifold of an unstable periodic orbit, this stable manifold being, at the same time, the basin boundary of the chaotic attractor [10,11]. Such a saddle is called a basin saddle since it lies on the basin boundary of the attractor and regions around such a saddle form escape regions for the chaotic trajectories resulting in nonchaotic behavior. Previous techniques for sustaining chaos have been designed around a feedback control mechanism in which a parameter or state variable was used to maintain chaos by reinjecting the dynamics into a region containing a chaotic saddle [1–3,12–14].

In contrast, the topology of the basin boundary saddle manifold structure may be used to design parameter control algorithms for sustaining chaos in parameter regimes where a crisis occurs [15,16]. Chaos is sustained by adjusting a system parameter discretely based on measuring a time series obtained from the system, and using embedding methods to reconstruct the dynamics in a phase space. Specifically, the system was treated as a black box and the dynamics reconstructed from time series measurements. Nonetheless, the above-mentioned techniques all make use of feedback information that must be gleaned from a measured time series. Implementing such schemes in practice can easily be done in systems that operate on very slow time scales, such as in Ref. [12], where operating frequencies are of the order of 1 Hz. Fast time scale applications, such as optical systems, require control interventions of the order of a 1-μs time scale to take place. Such control intervention, though not impossible, is difficult to implement in practice.

In the present paper we take a different approach to sustaining chaos. The approach still excites chaos, but it is an open-loop procedure that can be designed so that stable chaotic regions may be achieved in places where these were not stable previously. The procedure starts with a periodically driven system having a drive amplitude as an adjustable parameter. The drive amplitude is tuned so that the system operates in a crisis regime. The new feature we add is one of resonant amplitude modulation (am). That is, the amplitude fluctuates at half the primary frequency. Additionally, a phase difference between the amplitude modulation and primary frequency is considered as an extra parameter. The addition of the amplitude modulation allows extra manifold control at low energies in fast time scale systems. Moreover, it is easily implemented in a large class of experiments that are forced by an external drive frequency.

The advantage of our method is that we can initiate it without any knowledge of a crisis in a chaotic attractor. In our previous algorithms [15,16] accurate knowledge of the crisis region was necessary. Also the computational effort involved in our current approach is minimal since the time series analysis and phase-space reconstruction is not necessary any more. The parameter fluctuations used to sustain chaos in previous algorithms [1,2] required either faithful reconstruction of the phase space at the crisis or knowledge

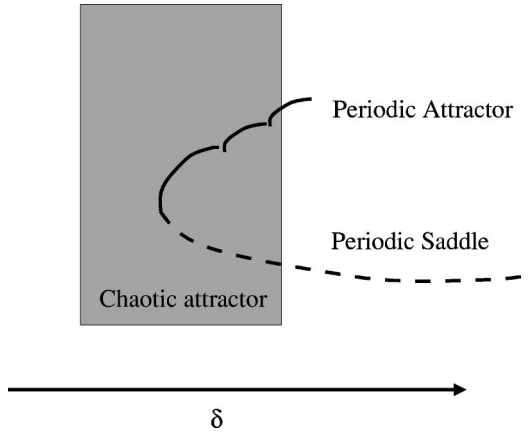

FIG. 1. A schematic picture illustrating the general bifurcation diagram. Coexisting chaotic and periodic attractors are shown, along with a branch of periodic saddles.

of the basin boundary of the chaotic attractor. In previous methods it was a delicate problem to re-excite chaos once the system settled to periodic behavior [16]. In the present approach this is no longer an issue due to the special design of the drive amplitude.

The paper is organized as follows. In the following section we present the general setup for multifrequency driving. We follow with a section on the CO_2 laser model that we worked with. In Sec. IV, we discuss the bifurcation structure of the model and analyze the control procedure from a perturbation analysis point of view. In Sec. V, we present numerical examples and the associated topology. We end the paper with a conclusion section that includes preliminary experimental results done on a driven CO_2 laser.

II. THE PROBLEM SETUP

To define the problem, we consider the general case of a dynamical system that is driven periodically. That is, if $F:R^n RI \rightarrow R^n$ is a vector field depending on time and a parameter δ lies in a bounded interval I, then the system we consider is

$$\frac{dx}{dt} = F(x,t,\delta), \tag{1}$$

where $F(x,t,\delta) = F(x,t+1,\delta)$. The solution to such a system is assumed to have a branch of periodic orbits of a given harmonic solution, which arises from a saddle node bifurcation. In addition, the bifurcation diagram goes through a period-doubling route to chaos via a crisis mitigated by the saddle branch of periodic orbits. That is, the saddle branch of orbits interacts with the chaotic attractor at some parameter value to cause a crisis in which the chaotic attractor disappears, and the remaining attractor window is a periodic orbit belonging to the attracting branch of the saddle-node bifurcation. (See Fig. 1 for the schematic picture.) In this paper, we assume that the unstable manifold of the periodic saddle branch is one dimensional.

So that control of some sort may be achieved within the drive amplitude parameter δ, we further assume that there is a subharmonic amplitude modulation. That is, we let $\delta = \delta_1[1+\delta_2 p(t+\phi)]$, where $p(t+2+\phi) = p(t+\phi)$. Specifically, we assume the amplitude modulation period is such that it is in resonance with the main drive. Here we assume that the frequency is 1/2 of the main drive frequency. We remark that in a previous paper, a 1:1 type of drive was used in a Melnikov analysis to create chaotic behavior [17]. However, it requires the use of a known unperturbed homoclinic orbit from which perturbation should occur [17], and as such is a local perturbation method. Finally, we introduce a relative phase ϕ as a second parameter, which we will adjust to control the bifurcations locally via period doubling, as well as globally via manifold crossings.

The assumption here is that chaos disappears due to a crisis, that is due to the interaction of the saddle manifolds with the chaotic attractor. In the case of quadratic nonlinearities used in modeling CO_2 lasers, it is the intersection of the stable and unstable manifolds that cause a complete destruction of the basin of attraction of the chaotic attractor, resulting in a globally attracting periodic attractor. This phenomenon is universal, as long as the unstable manifold of the saddle branch is one dimensional in Ref. [11]. We now describe our physical model in which we detail our analysis.

III. THE AMPLITUDE MODULATION LASER MODEL

We consider the laser rate equations for a single mode, homogeneously broadened modulated laser, modeled by the intensity I and population inversion D. The periodic modulations of the cavity decay rate are modeled by $\kappa(t') = \kappa_0[1+\Delta\cos(\sigma t')]$, where Δ and σ are the amplitude and frequency of the modulations, respectively. By rescaling time by letting $s = \kappa_0 t'$, the equations governing the time behavior are

$$\frac{dI}{ds} = 2I[-1+AD-\Delta\cos(\Omega s)],$$

$$\frac{dD}{ds} = \gamma[1-D(1+I)]. \tag{2}$$

Here A is the pump parameter and $\gamma = \gamma_\parallel/\kappa_0$ is the loss rate for the population scaled by the cavity decay rate $\Omega = \sigma/\kappa_0$. We rescale the problem following Ref. [18] by shifting the steady solution to the origin, and rescaling the state variables and time we obtain

$$\frac{dx}{dt} = -y - \epsilon x(a+by),$$

$$\frac{dy}{dt} = (1+y)[x-\delta(t)\cos(\omega t)]. \tag{3}$$

We let $\epsilon_1 = \epsilon(a+b)$ and $\epsilon_2 = \epsilon b$, where $1+y$ and x denote (scaled) intensity and population inversion. In Eq. (3), $\delta(t) = \delta_1[1+\delta_2\cos(\omega/2+\phi)]$, so that the amplitude modulation is in a 1:2 resonance with respect to the cavity drive. This will satisfy the above hypotheses in Eq. (1).

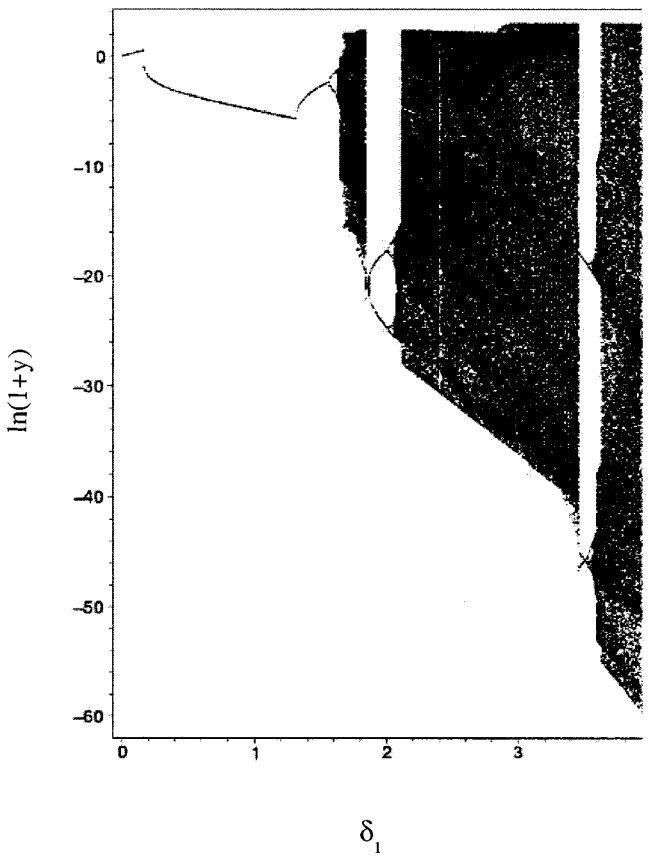

FIG. 2. A bifurcation diagram showing the attractors $\ln(1+y)$ of Eq. (3) as a function of δ_1. The sampling was done at half the drive frequency, with only the primary drive frequency being active. The abrupt widening of the attractors denotes boundary crises, where stable manifold boundaries intersect with the attractors. See Ref. [11] for details, which shows that the hypotheses of Eq. (1) are satisfied. The axes are dimensionless quantities defined by Eqs. (3).

When $\delta_2=0$, Eq. (3) acts as a damped driven nonlinear oscillator, where the drive is at frequency ω. If we fix $\epsilon_1=0.09$ and $\epsilon_2=0.003$, we identify the crisis regime by using δ_1 as the bifurcation parameter. In Fig. 2, we see that as δ_1 varies, a period doubling route to chaos occurs and coexists with a period-2 attractor that emanates from a saddle-node bifurcation. It is well known that the period-2 saddle causes the destruction of the chaotic attractor. The result is that after the crisis a chaotic saddle exists along with a period attractor.

Therefore, coexisting with the chaotic attractor is a branch of periodic orbits of period-2 emanating from a saddle-node bifurcation point. The period-2 saddle mitigates the crisis. A similar saddle node of period 3 similarly controls the period-3 crisis. We examine the structure of bifurcations and manifolds in the presence of subharmonic amplitude modulations.

The chaotic attractor disappears as the direct result of the topology of the manifolds corresponding to the period-2 saddle. For reference purposes, we show the topology of the manifolds just after the crisis occurs, as shown in Fig. 3. There is only a periodic attractor (of period 4) in the figure. The stable manifold separates the attractor from a chaotic transient when the initial conditions start near the chaotic

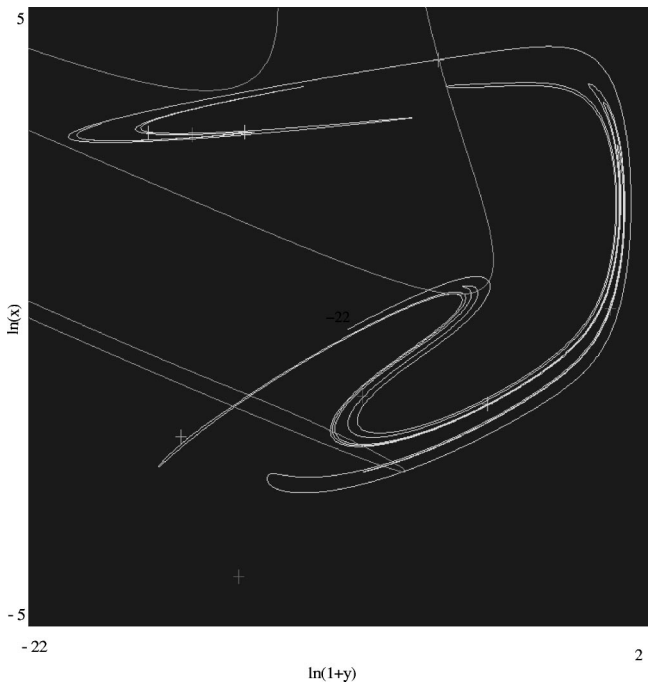

FIG. 3. The picture illustrates the manifold structure just past a crisis value at $\delta_1=1.9$ where the phase space is strobed at the primary forcing frequency. The only attractor present is a period-4 attractor. The chaos is transient due to the intersection of the unstable and stable manifolds of the period-2 saddle. The axes are dimenionless quantities defined by Eqs. (3).

saddle. (See Ref. [15] for details.) By varying fluctuations about the base parameter δ_1, it is known that if one monitors the region about the saddle, a closed loop method of sustaining chaos can be done to excite a chaotic saddle [12,15]. However, it is most difficult to implement in optical systems, since the control loop has to sample and respond rapidly, of the order of a microsecond. Therefore, we examine the structure of bifurcations and manifolds in the presence of subharmonic amplitude modulations.

IV. PERIOD-DOUBLING MODIFICATION

The effect of the amplitude modulation at half the frequency is expected to play a role in the global bifurcations of the CO_2 laser. Although the main goal is to manipulate the manifold intersections of a mitigating saddle orbit, no current analytic method exist to handle the class of dynamic models with quadratic nonlinearities. However, as stable and unstable manifolds of that saddle come to intersect as a function of a parameter, it is numerically verified that the location of a period-doubling bifurcation off a stable branch also changes. Therefore, in this section we show how the subharmonic amplitude modulation changes the period-doubling bifurcation point as a function of amplitude and phase.

Consider Eq. (3) where

$$\delta(t)=\delta_1[1+\delta_2(\omega_2 t+\phi)]. \tag{4}$$

Since the chaotic saddles that occur in the crisis regions occur as the result of primary saddle-node bifurcations [11],

they contain oscillations of large pulse amplitude. We examine the large amplitude pulsations by deriving a Poincaré map. The surface of section is defined as when the population inversion reaches its minimum value, just after the emission of a pulse where the intensity is small ($y \approx 0$). The method used to derive the map for the laser was first presented in Ref. [18] for the case of $\epsilon = 0$ (no damping) and $\delta_2 = 0$ (single-frequency modulation). The authors were able to accurately locate period-doubling bifurcations of the periodic subharmonic-resonance solutions. The map has been extended by Carr and co-workers [19,20] to account for dissipation. The saddle-node bifurcation to periodic solutions could be determined in addition to the period-doubling bifurcations. Newell *et al.* [21] used a similar map to examine a two-frequency modulation. However, in their case the two modulations acted independently and were not in the am configuration.

For the present analysis we ignore the effects of dissipation by setting $\epsilon = 0$, and focus on how the AM modulation effects the period-doubling bifurcation of the primary resonances. The map is derived in the same way as in Ref. [18] and we obtain

$$t_{n+1} = t_n - 2x_n, \tag{5}$$

$$x_{n+1} = x_n + 2\,\delta(t_{n+1})\cos(\omega_1 t_{n+1}), \tag{6}$$

where $\omega_1 = \omega$ is the primary modulation frequency. The time t_n is when the inversion reaches its minimum x_n on the periodic orbit. Periodic orbits of Eq. (3) are fixed points of the map (5) defined by $x_{n+1} = x_n = x_p$ and $t_{n+1} = t_n + P$, where P is defined as the period. The fixed point conditions are substituted into the map (5) to obtain

$$t_n = \pm\frac{\pi}{2} + nP, \quad P = \frac{2\pi m}{\omega_1} \ (m \text{ is an integer}), \quad x_p = -\frac{P}{2}. \tag{7}$$

The results are the same as for the case of only a single modulation. Subharmonic resonances are differentiated by the parameter $m = 1,2,\ldots$. The phase $\pm(\pi/2)$ indicates there are two solutions. These appear through a saddle-node bifurcation that in the presence of dissipation ($\epsilon \neq 0$) occurs for nonzero forcing ($\delta_1 \neq 0$).

Period-doubled solutions are defined by the conditions $x_{n+2} = x_n$ and $t_{n+1} = t_n + 2P$. The two conditions that describe the period-doubled solutions are implicit and difficult to analyze in general. However, progress is possible if we examine close to the period-doubling bifurcation. This is accomplished by setting

$$t_{n+2} - t_{n+1} = P + \tau, \quad t_{n+1} - t_n = P - \tau. \tag{8}$$

The period-doubling bifurcation is defined by $\tau = 0$ and $t_{n+1} = t_n$. We consider $\tau \ll 1$ and assume that the am modulation term is a small perturbation to the primary modulation. Assuming expansions of t_n, δ_1, δ_2 in τ along with the period-doubling conditions (8) are substituted into the map (5) we analyze at each order or τ.

The period-doubling results depend on the relationship between the primary frequency ω_1 and the am modulation frequency ω_2. We consider the simplest cases of $\omega_2 = \omega_1/2$ and $\omega_2 = l\omega_1$, where l is an integer, to obtain a bifurcation equation that relates the modulation amplitude to the period.

When $\omega_2 = l\omega_1$, l is an integer, or when $l = \frac{1}{2}$, m is even, the bifurcation equation is the same and is given by

$$\delta_1 = \frac{1}{\omega_1} - \frac{\delta_2}{\omega_1}\cos\left(-\frac{\pi}{2}\omega_2 + \phi\right) + \frac{\delta_2^2}{\omega_1}\cos^2\left(-\frac{\pi}{2}\omega_2 + \phi\right) + \frac{1}{24}\omega_1\tau^2 + O(\tau^3). \tag{9}$$

If there is no am modulation, $\delta_2 = 0$ and we recover the results of Schwartz and Erneux [18]. The am modulation is a constant with respect to τ. Hence, it causes a shift in the period-doubling bifurcation point ($\tau = 0$) from $\delta_1 = 1/\omega_1$ to $\delta_1 = (1/\omega_1) + O(\delta_2)$. The phase ϕ effects not only the magnitude of the shift but also whether the bifurcation is advanced or delayed. This agrees with the phase effects on the global manifold crossings below.

When $l = \frac{1}{2}$, m is odd, we obtain a different bifurcation result ($\omega_2 = \omega_1/2$, but the primary resonance has odd $= m$). In this case the bifurcation equation is given by

$$\delta_1 = \frac{1}{\omega_1} + \left[\frac{\delta_2}{4}\sin\left(-\frac{\pi}{2}\omega_2 + \phi\right)\right]\tau + \frac{1}{24}\omega_1\tau^2 + O(\tau^3). \tag{10}$$

The am modulation produces a term linear in τ. This causes a shift of the period-doubling branch of solutions off the primary branch. The local bifurcation is no longer a pitch fork but transcritical. Also, there is now an $O(\delta_2\tau)$ region of bistability between the period-doubled branch and the original subharmonic resonance.

Finally, we note that the shift in the bifurcation curves caused by the am modulation are different than the case of two independent modulation frequencies, which were studied in Ref. [21]. There the perturbation resulted in the destruction of the bifurcation point and an imperfect bifurcation results. For an imperfect bifurcation there is a smooth transition from the primary to secondary branch instead of a definite bifurcation point.

The above analysis shows how the amplitude and phase of the am modulation shifts the period-doubling bifurcation of the subharmonic resonances and changes the topology of the bifurcation. This will have a direct effect on the topology of the phase space as a whole and effect the transverse crossings of manifolds. While the analysis cannot directly describe the change in manifold crossings, it can be used to estimate the parameter values such that manifold crossings may be analyzed numerically. This is done in the following section.

V. NUMERICAL RESULTS OF AMPLITUDE MODULATION

Since the amplitude and phase modulation of the second harmonic predicts a shift in the location of the period-

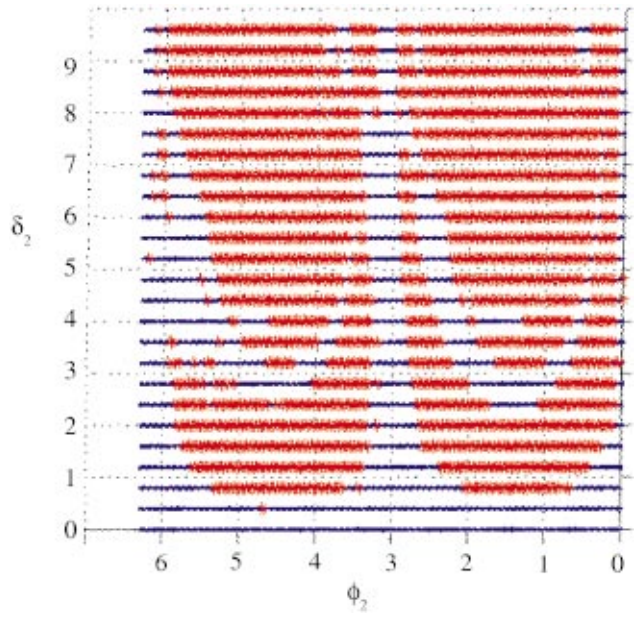

FIG. 4. (Color) A figure depicting excited chaotic (red) and nonchaotic (blue) regions as a function of δ_2 and ϕ. The parameters for δ_1, ϵ_1, and ϵ_2 in Eq. (3) are chosen in the first crisis region, as in Fig. 3. See text for details.

doubling branch off the primary periodic branch of orbits, it is reasonable to expect that global changes in the relative positions of the stable and unstable manifolds of the saddle change as well. We consider the full amplitude modulation model given in Eqs. (3), where we compute solutions as a function of amplitude and phase of the subharmonic resonance term. The fixed parameters are tuned so that variations in amplitude and phase are referred to the control manifolds in Fig. 3 where only a globally attracting orbit exists. The results are shown in Fig. 4. Notice there are two regions consisting of two distinct lobes in which chaos can be excited. We now examine the manifold intersections of the governing saddle orbits in each of the two regions: the red region and the blue region.

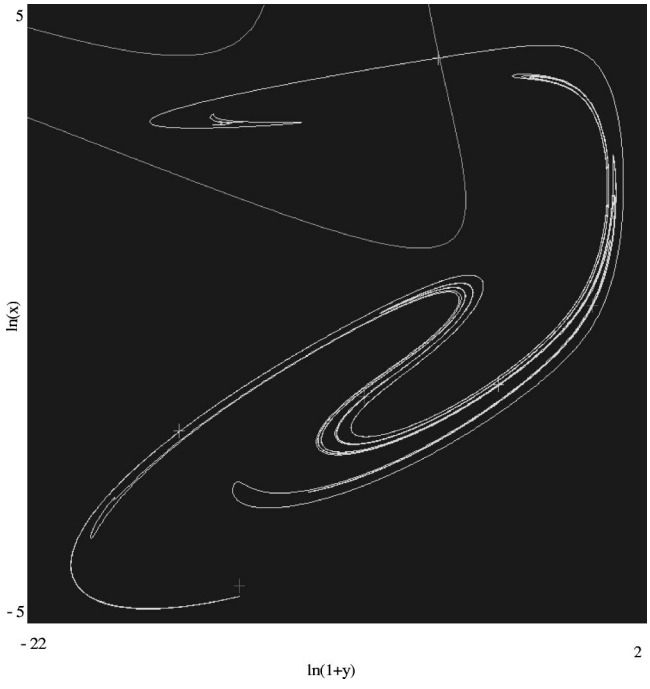

FIG. 5. Manifold picture at the crisis value $\delta=1.9$ for amplitude and phase chosen in the red region in Fig. 4. $\delta_2=0.2$ and $\phi=0.5$. The situation is that of bistability, where the chaotic attractor coexists with the periodic attractor. The axes are dimenionless quantities defined by Eqs. (3).

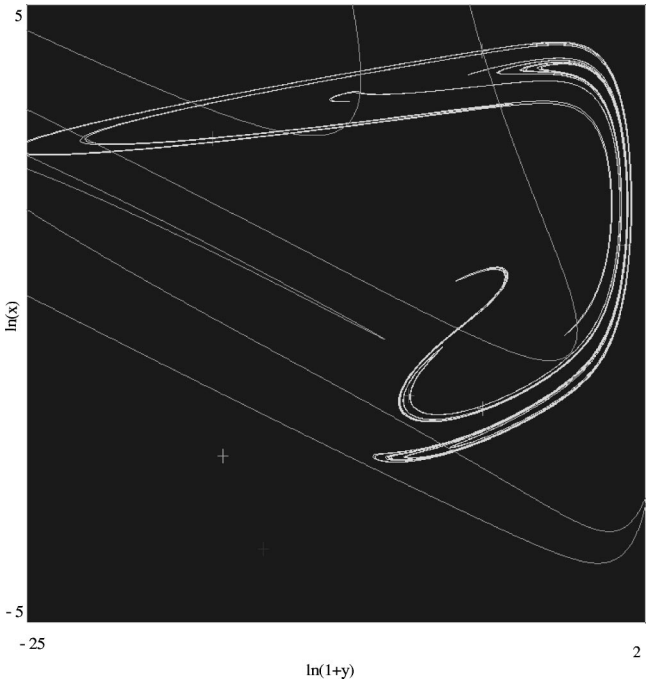

FIG. 6. Manifold picture when open-loop control is applied. There exists a unique chaotic attractor when the amplitude and phase are chosen in the red region of Fig. 4. $\delta_2=0.2$ and $\phi=4.75$. The axes are dimenionless quantities defined by Eqs. (3).

As it can be seen in Fig. 4, chaotic regions are clearly excited (regions in red). However, in addition to the chaotic attractors, there coexists a periodic attractor (blue region). That is, the chaotic attractor is not the unique attractor, and therefore, the amplitude and the phase must be chosen appropriately in order to excite the chaotic transient. The reason multiple attractors coexist is due to the noncrossing of the stable and unstable manifolds of the period-2 saddle, as given in Fig. 5. The situation is quite similar to that of the bistable parameter regions in the absence of any amplitude modulation. That is, the stable manifold is the distinct basin boundary separating the periodic and chaotic attractors.

In contrast, when applying open-loop control there exists a global chaotic attractor for values of the drive parameters corresponding to red regions in Fig. 3. The manifolds are presented in Fig. 6. Notice that in addition to the unstable manifold intersecting the stable manifold from the right, the unstable manifold to the left of the saddle cuts through all basins. That is, there exists only one chaotic attractor for parameters chosen in the red lobe regions.

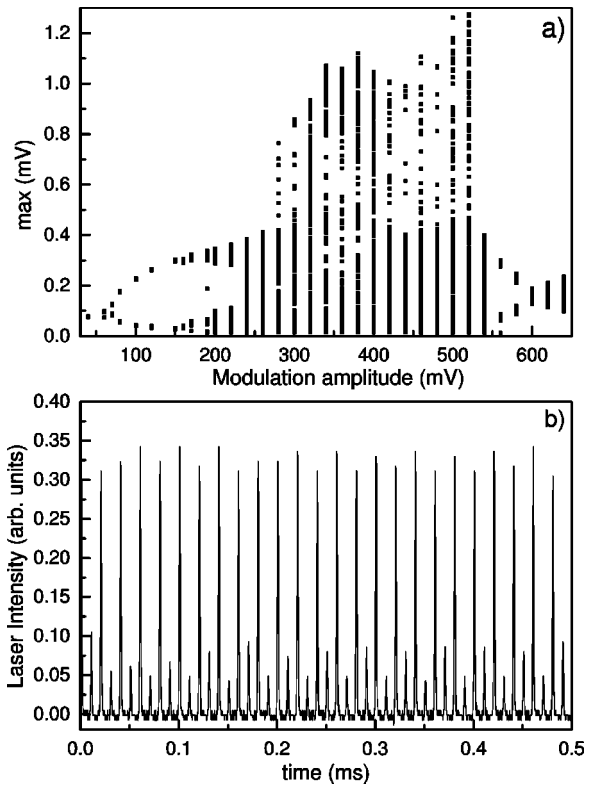

FIG. 7. A bifurcation picture from a CO_2 laser experiment. Plotted is the laser intensity strobed at the primary frequency as a function of the modulation amplitude (top panel). In the crisis regime, the laser intensity as a function of time shows periodic behavior only (bottom panel).

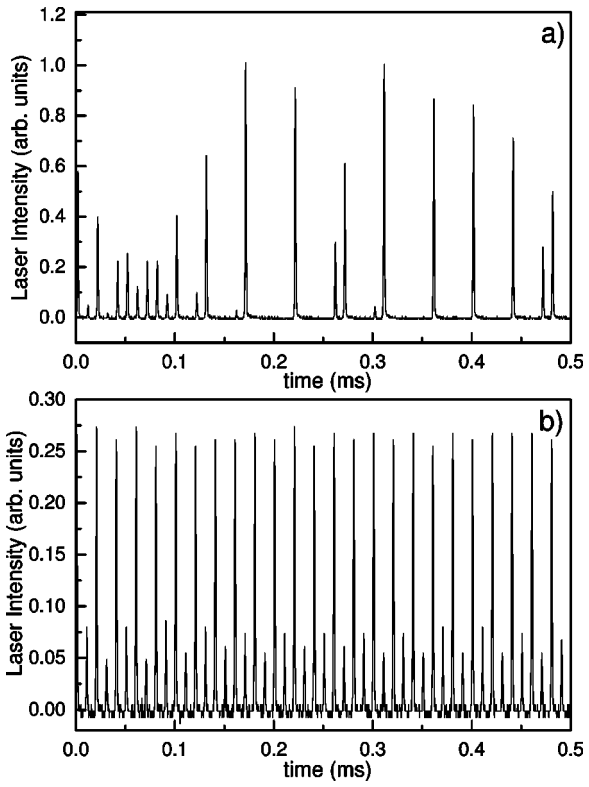

FIG. 8. Time evolution of the laser intensity when an amplitude modulation of 0.01 is applied to the periodic behavior (shown in Fig. 7) emerging after the crisis. In the top panel, the phase of the applied perturbation is $0.1\times 2\pi$ and it continously reexcites chaotic transients. In the bottom panel, the phase is $0.4\times 2\pi$. In such a case, only a slight modification of the periodic behavior is produced.

VI. DISCUSSION

We have presented an open-loop control procedure to induce chaos. The procedure can equally well induce periodic behavior in chaotic regions using the same type of parameter sweep. The method is based on driving the system with a 1:2 resonance modulation and varying the amplitude and the phase of the drive in this modulation. The method is general and can be applied to any periodically driven dynamical system that exhibits regions of chaos in its dynamics. The type of control we propose will access these regions. The system was applied to a two-level periodically driven CO_2 laser model. It works equally well on higher-dimensional models that are going to be addressed in forthcoming papers. Moreover, the chaotic regions that can be generated exhibit a universal character, in the sense that they are qualitatively similar in various models, as it will be shown in forthcoming papers. The success of inducing chaos was explained by the change in topology that occurs: at a crisis the horseshoe dynamics that sustains chaos destabilizes and only chaotic transients remain. By implementing amplitude modulation in a 1:2 resonance, the topological structure about the saddle which is accountable for the disappearance of the chaotic attractor is recreated making chaos possible. The method is easy to implement in experiments since it does not require embedding methods applied at the crisis region as in previous algorithms.

Finally we show a preliminary CO_2 laser experiment in which the above ideas have been tested. Details of the full experiment will be presented elsewhere. In Fig. 7, a bifurcation picture of a CO_2 laser experiment shows the initial bifurcation prior to turning on the amplitude modulation. The crisis region in which only periodic behavior occurs is shown as a time series in panel (b).

The frequency at which the laser was modulated was 100 kHz. To see if the manifold ideas work, we turned on the amplitude forcing at 50 kHz, and varied the amplitude and phase. The preliminary results for two distinct behaviors are shown below in Fig. 8. In both panels the amplitude modulation is fixed at 0.01. The two pictures show two different phases applied to the amplitude modulation. In panel (a), the phase was set at $\phi=0.1$, which generates chaotic bursting. In panel (b), the phase $\phi=0.4$ generated periodic behavior. The experiment, although preliminary, does generate the correct type of behavior based on the theory.

ACKNOWLEDGMENTS

I.B.S. and I.T. were supported by the Office of Naval Research, T.C. was supported by the National Science Foundation through Grant No. DMS-9803207, and R.M. was suppoted by EC Project No. HPRN CT 2000 00158. We also would like to thank E. Allaria for collecting the experimental measurements.

[1] W. Yang, M. Ding, A.J. Mandell, and E. Ott, Phys. Rev. E **51**, 102 (1995).
[2] V. In *et al.*, Chaos **7**, 605 (1997).
[3] M. Dhamala and Y.-C. Lai, Phys. Rev. E **59**, 1646 (1999).
[4] G.D. VanWiggeren and R. Roy, Science **279**, 1198 (1998).
[5] I.T. Georgiou and I.B. Schwartz, SIAM (Soc. Ind. Appl. Math.) J. Appl. Math. **59**, 1178 (1999).
[6] I.B. Schwartz and I.T. Georgiou, Phys. Lett. A **242**, 307 (1998).
[7] Ary L. Goldberger, in Proceedings of the First Experimental Chaos Conference, edited by Sandeep Vohra *et al.* (1991).
[8] S.J. Schiff, K. Jerger, D.H. Duong, T. Chang, M.L. Spano, and W.L. Ditto, Nature (London) **370**, 615 (1994).
[9] C. Grebogi, E. Ott, and J.A. Yorke, Physica D **7**, 181 (1983).
[10] K. T. Alligood, T. D. Sauer, and J. A. Yorke, *Chaos* (Springer-Verlag, New York, 1997).
[11] I.B. Schwartz, Phys. Rev. Lett. **60**, 1359 (1988).
[12] V. In, M. Spano, and M. Ding, Phys. Rev. Lett. **80**, 700 (1998).
[13] V. In, S.E. Mahan, W.L. Ditto, and M.L. Spano, Phys. Rev. Lett. **74**, 4420 (1995).
[14] S. Codreanu, Chaos, Solitons Fractals **13**, 839 (2002).
[15] I.B. Schwartz and I. Triandaf, Phys. Rev. Lett. **77**, 4740 (1996).
[16] I. Triandaf and I.B. Schwartz, Phys. Rev. E **62**, 3529 (2000).
[17] R. Chacon, Phys. Rev. Lett. **86**, 1737 (2001).
[18] I. Schwartz and T. Erneux, SIAM (Soc. Ind. Appl. Math.) J. Appl. Math. **54**, 1083 (1994)
[19] I.B. Schwartz and T.W. Carr, Phys. Rev. E **59**, 6658 (1999).
[20] T.W. Carr, L. Billings, I.B. Schwartz, and I. Triandaf, Physica D **147**, 59 (2000).
[21] T.C. Newell, A. Gavrielides, V. Kovanis, D. Sukow, T. Erneux, and S.A. Glasgow, Phys. Rev. E **56**, 7223 (1997).